

XMM-Newton and *Chandra* observations of the globular cluster NGC 6388

A. A. Nucita¹, F. De Paolis², G. Ingrassio², S. Carpano¹, and M. Guainazzi¹

¹ XMM-Newton Science Operations Centre, ESAC, ESA, PO Box 78, 28691 Villanueva de la Cañada, Madrid, Spain

² Dipartimento di Fisica, Università del Salento, and INFN, Sezione di Lecce, CP 193, 73100 Lecce, Italy
e-mail: nucita@le.infn.it

Received 15 October 2007 / Accepted 27 November 2007

ABSTRACT

Context. By studying the optical brightness surface density of the globular cluster NGC 6388, it has been recently proposed that it harbors a central intermediate-mass black hole with mass $\approx 5.7 \times 10^3 M_{\odot}$.

Aims. We expect that the compact object in the center of NGC 6388 emits radiation in the X-ray band as a consequence of the accretion from the surrounding matter. We searched for XMM-Newton and Chandra observations towards NGC 6388 to test this hypothesis.

Methods. We determine both the hardness ratios and luminosity with a minimum set of assumptions for each of the identified field sources.

Results. The Chandra satellite disentangles several point-like X-ray sources, probably low mass X-ray binaries, well within the core radius of the globular cluster. However, three of them, coinciding with the cluster center of gravity, remain unresolved. Their total luminosity is $L_X^{\text{Obs}} \approx 2.7 \times 10^{33} \text{ erg s}^{-1}$. If one of these sources is the X-ray counterpart of the intermediate-mass black hole in NGC 6388, the corresponding upper limit on the accretion efficiency, with respect to the Eddington luminosity, is 3×10^{-9} . This measurement could be tightened if moderately deep radio observations of the field were performed.

Key words. Galaxy: globular clusters: general – Galaxy: globular clusters: individual: NGC 6388

1. Introduction

Over the last few years, several pieces of evidence have been accumulated pointing to the presence of an intermediate-mass black hole (hereafter IMBH) with mass $\approx 10^3 M_{\odot}$ in a globular cluster. The first evidence comes from the extrapolation to globular clusters of the $M_{\text{BH}} - M_{\text{Bulge}}$ relation found for super massive black holes in galactic nuclei (for details see Magorrian et al. 1998), which leads to the prediction of the existence of IMBHs.

The second hint is related to the discovery of the so called ULXs, i.e. ultra-luminous, compact X-ray sources (with luminosity greater than $\sim 10^{39} \text{ erg s}^{-1}$), which are believed to be IMBHs rather than binaries containing a normal stellar mass black hole (Miller & Colbert 2003).

More indirect evidence of the existence of IMBHs comes from the study of the central velocity dispersion of stars in specific globular clusters. For example, by using the velocity dispersion measurements, Gerssen et al. (2002, 2003), and Gebhardt et al. (2002, but see also Pooley & Rappaport 2006) proposed that IMBHs may exist in M 15 and G1 (an M 31 globular cluster) with masses about $10^3 - 10^4 M_{\odot}$ ¹.

Objects of the IMBH size are predicted by detailed N -body simulations (see e.g. Portegies Zwart et al. 2004), according to which an IMBH forms as a consequence of merging of massive

stars. Furthermore, at least for the cases of M 15 and 47 Tucane, the precise measurements of P and \dot{P} of four millisecond pulsars (with negative \dot{P}) has allowed De Paolis et al. (1996) to put rather stringent upper limits to the mass of the central black hole of $\sim 10^3 M_{\odot}$.

In addition to the previous evidence, it is also expected that globular clusters with a central IMBH are characterized by a cusp in the inner stellar density profile (i.e. $\rho \propto r^{-7/4}$), so that the projected density profile, as well as the surface brightness, should also have a cusp with slope $-3/4$. As shown by Miocchi (2007), the globular clusters that most likely harbor an IMBH are those having the projected photometry well fitted by a King profile, except in the central part where a power law deviation ($\alpha \approx -0.2$) from a flat behavior is expected. However, as pointed out by Baumgardt et al. (2003, 2003), a similar behavior is also expected in a constant core density King profile ($\alpha \approx 0$) when the mass segregation effect of stellar remnants is considered. This explanation, however, is uncertain because it depends on the assumption that all the neutron stars and/or stellar mass black holes are retained in the cluster so that the existence of a central IMBH cannot be completely ruled out (see Gebhardt et al. 2005). On the other hand, the errors with which the slopes of central densities can be determined are of the order 0.1–0.2 (Noyola & Gebhardt 2006), so that surface density profiles do not give clear evidence of the existence of IMBH in globular clusters, thus requiring observations in different bands.

Among all the known globular clusters in our Galaxy, NGC 6388 is one of the best candidates to host an IMBH (Baumgardt et al. 2005). NGC 6388 is a globular cluster at distance $d \approx 11.5 \text{ kpc}$ (with center at coordinates

¹ The observed brightness and the velocity dispersion profiles of the G1 (Baumgardt et al. 2003) and M 15 (Baumgardt et al. 2003) globular clusters can be well fitted by usual evolutionary King models. When the mass segregation effect is taken into account, a sharp increase in the mass-to-light ratio towards the cluster core is found, thus avoiding the necessity of a central IMBH.

AR = $17^{\text{h}}36^{\text{m}}17.6^{\text{s}}$, Dec = $-44^{\circ}44'08.2''$) and with an estimated mass of $2.6 \times 10^6 M_{\odot}$ (Lanzoni et al. 2007). By using a combination of high resolution (HST ACS-HCR, ACS-WCS and WFPC2) and wide-field (ESO-WFI) observations, Lanzoni et al. (2007) derived the center of gravity, the projected density profile and the central surface brightness profile of NGC 6388. While the overall projected profile is well fitted by a King model (with concentration parameter $c = 1.8$ and core radius $r_c \approx 7.2''$), a significant power law (with slope $\alpha \approx -0.2$) deviation from a flat core behavior has been detected within $\approx 1''$. This was interpreted as the signature of the existence of an IMBH with mass $\approx 5.7 \times 10^3 M_{\odot}$ at the center of NGC 6388. We expect that the central IMBH emits significant radiation in the X-ray band as a consequence of the accretion of the surrounding matter. Thus, we searched for both *XMM-Newton* and *Chandra* observations towards the globular cluster NGC 6388.

The paper is structured as follows: in Sect. 2, we briefly describe the *XMM-Newton* and *Chandra* observations and data reduction. In Sect. 3, we describe the main characteristics of the sources detected within a few core radii of the globular cluster and in Sect. 4 we address our main results and conclusions.

2. *XMM-Newton* and *Chandra* observation and data reduction

The globular cluster NGC 6388 was observed in March 2003 (observation ID 0146420101) with both the EPIC MOS and PN cameras (Turner et al. 2001; Strüder et al. 2001) operating with the medium filter mode. The EPIC observation data files (ODFs) were processed using the *XMM-Science Analysis System* (SAS version 7.0.0). Using the latest calibration constituent files currently available, we processed the raw data with the *emchain* and *epchain* tools to generate event lists. After screening with standard criteria, as recommended by the Science Operation Centre technical note XMM-PS-TN-43 v3.0, we rejected any time period affected by soft proton flares. The remaining time intervals resulted in effective exposures of $\approx 2.5 \times 10^4$ ks, $\approx 2.4 \times 10^4$ ks, and $\approx 1.3 \times 10^4$ ks for MOS 1, MOS 2, and PN, respectively.

In Fig. 1, the *XMM-Newton* observed field of view (PN camera) is shown. The green circle is centered on NGC 6388 and has a radius equal to the half mass radius of the globular cluster. The source spectra were extracted in a circular region centered on the nominal position of the target in the three EPIC cameras, while the background spectra were accumulated in annuli around the same coordinates. The resulting spectra were rebinned to have at least 25 counts per energy bin.

The spectra were simultaneously fitted with XSPEC (version 12.0.0). In Fig. 2, we show the MOS 1, MOS 2, and PN spectra for NGC 6388 and the respective fits. The best-fitting model was an absorbed power law ($\chi^2/\nu = 1.14$ for $\nu = 147$). We left all the parameters free, yielding $N_{\text{H}} = 2.7^{+0.3}_{-0.3} \times 10^{21} \text{ cm}^{-2}$, $\Gamma = 2.4^{+0.1}_{-0.1}$ and $N = 2.2^{+0.2}_{-0.2} \times 10^{-4}$ for the column density², power law index and normalization, respectively.

The flux in the 0.5–7 keV is $F_{0.5-7} = 4.0^{+0.2}_{-0.2} \times 10^{-13} \text{ erg cm}^{-2} \text{ s}^{-1}$ which, for the globular cluster distance of ~ 11.5 kpc, corresponds to a luminosity of $L_{0.5-7} \approx 6.31 \times 10^{33} \text{ erg s}^{-1}$. Note that all the uncertainties quoted above are given at a 90% confidence level.

² Within the error, the column density obtained from the fit procedure is compatible with that due to gas in our Galaxy along the line-of-sight to NGC 6388, i.e. $N_{\text{H}} \approx 2.5 \times 10^{21} \text{ cm}^{-2}$ (Dickey & Lockman 1990).

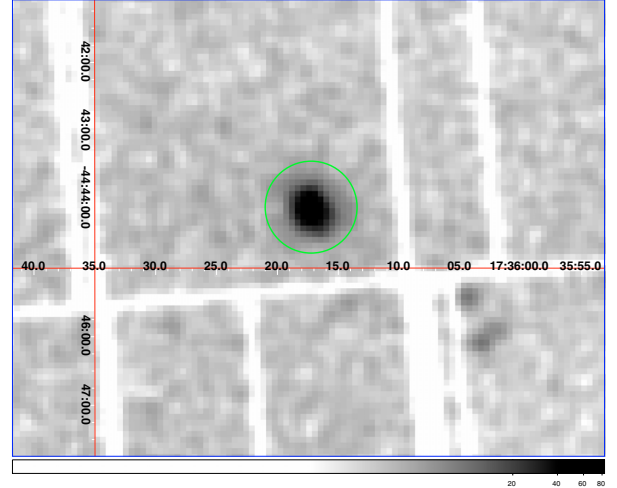


Fig. 1. The *XMM-Newton* field of view (PN camera) centered on NGC 6388. The green circle has a radius comparable to the half mass radius ($\approx 0.67''$) of the globular cluster. (This figure is available in color in electronic form.)

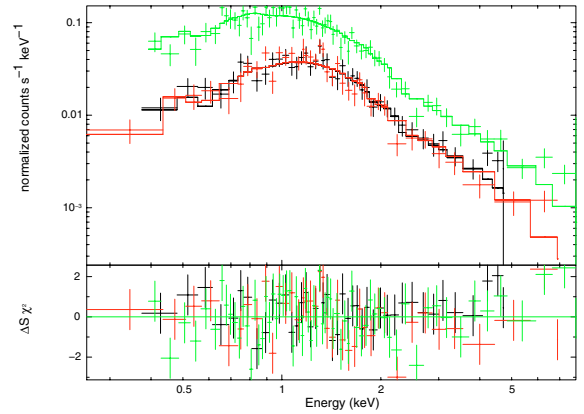


Fig. 2. The simultaneous fit to the MOS 1 (red), MOS 2 (black), and PN (green) data with a model based on an absorbed power law (see text for more details). (This figure is available in color in electronic form.)

The information that we can get from *XMM-Newton* data are important in obtaining an overall description of the X-ray radiation coming from NGC 6388. However, the *Chandra* satellite has a much better angular resolution than the *XMM-Newton* telescope and therefore it is worth using *Chandra* to verify whether the emission detected by *XMM-Newton* is due to a single source rather than superpositions of several bright X-ray sources.

The globular cluster was observed by *Chandra* with the ACIS-S camera (for ≈ 45 ks, observation ID 5505). In our analysis, we used the event 2-type files and followed the standard procedures for analysis of *Chandra* data using the CIAO version 3.4 tool suite. The background level during the observation was nominal.

We created images in the full (F = 0.5–7 keV), soft (S = 0.5–1.5 keV), medium (M = 1.5–2.5 keV) and hard (H = 2.5–7 keV) bands, and created a true color X-ray image of the globular cluster (given in Fig. 3). The X-ray emission towards NGC 6388 detected by the *XMM-Newton* satellite is associated with several discrete sources.

We searched in the images in each band for discrete sources by using the CIAO *celldetect* tool with a threshold signal-to-noise detection value of 3. In the following, we will treat only

Table 1. We report some useful parameters for the globular cluster NGC 6388 as given in Harris (1996). The columns represent the distance to NGC 6388, the core radius, the half mass radius, the central luminosity density, the concentration as derived by a King fit to the photometric data, the total magnitude and mass.

D (kpc)	R_c (arcmin)	R_H (arcmin)	$\log(\rho_c)$ (L_\odot/pc^3)	c	V_t	M ($\times 10^6 M_\odot$)
11.5	0.12	0.67	5.29	0.17	6.72	2.6

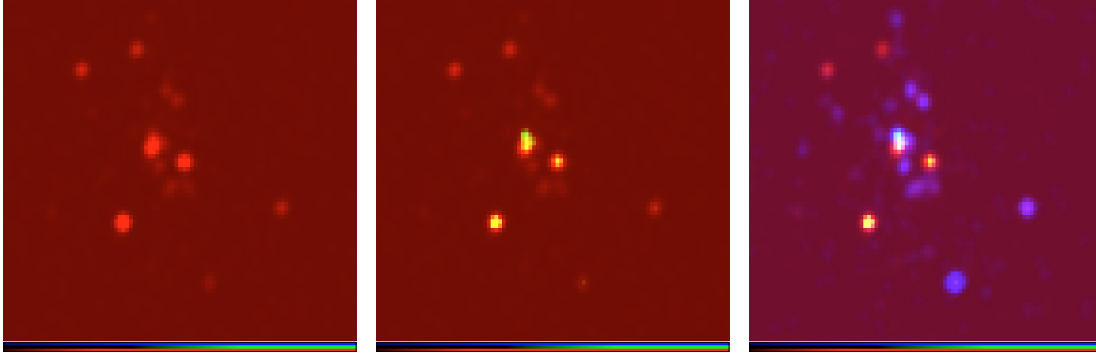


Fig. 3. *Chandra*/ACIS images in the soft, medium and hard bands. From the left to the right, the soft, soft+medium and soft+medium+hard images are shown. (This figure is available in color in electronic form.)

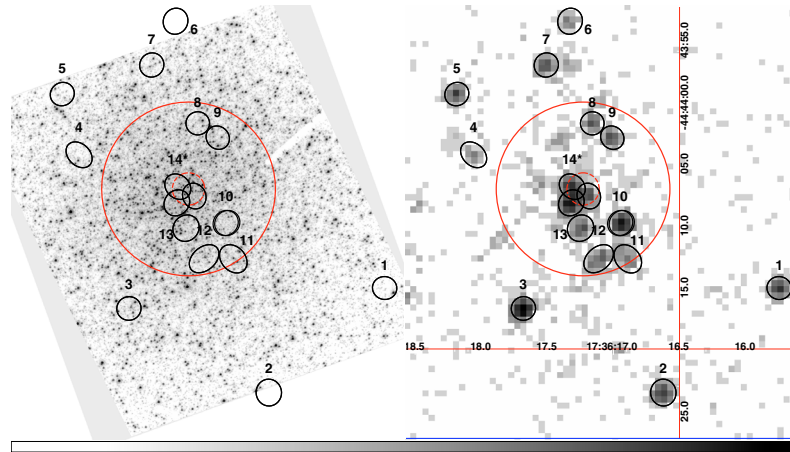


Fig. 4. A comparison of the *Chandra* and HST ACS-HRC fields of view towards NGC 6388 is given. The red solid circles represent the globular cluster core with radius $\approx 7.2''$, while the red dashed circles ($\approx 1.3''$) are centered on the center of gravity (see text for more details). (This figure is available in color in electronic form.)

the sources detected within ~ 2 core radii from the NGC 6388 center. This resulted in the detection of 16 discrete sources well within the half mass radius ($\approx 40''$) of NGC 6388. Of the detected sources, 9 are contained within the globular cluster core radius ($\approx 7''$), while 3 are close to the NGC 6388 center of gravity, which is located at $\text{AR} = 17^{\text{h}}36^{\text{m}}17.23^{\text{s}}$ and $\text{Dec} = -44^{\circ}44'07.1''$ (Lanzoni et al. 2007) with an uncertainty of $\approx 0.3''$ in both coordinates. The absolute errors associated with *Chandra* astrometry is $\approx 1''$.

The detected X-ray sources appear to be associated with the globular cluster NGC 6388. Based on the $\text{Log } N - \text{Log } S$ relationship of Giacconi et al. (2001), the estimated number of the background sources (with flux greater than the minimum detected flux, i.e. $\approx 8 \times 10^{-15} \text{ erg cm}^{-2} \text{ s}^{-1}$) contained within the cluster half mass radius is $\approx 10^{-2}$.

In Fig. 4, we show the detected discrete sources in the *Chandra* 0.5–7 keV image (right panel) as the encircled ones (each source being labeled with an increasing number). In left panel of the same figure, we show a $29.1'' \times 28.4''$ HST ACS-HRC image (filter *V F555W*) of the same field of view. The red

solid circle represents the NGC 6388 core, while the dashed circle is centered on the globular cluster center of gravity and has a radius of $\approx 1.3''$ as the sum of the uncertainties of the center of gravity and the absolute position error of *Chandra*.

We estimated the counts of each source from an aperture including most of the observed emission³. The background has been estimated by using annuli around each source when possible, or circles with the same extraction region radius otherwise (excluding any encompassed source).

For each source, we extracted the net number of counts in the full band and evaluated the hardness ratios $\text{HR1} = (S - M)/(S + M)$, $\text{HR2} = (M - H)/(M + H)$ and $\text{HR3} = (S - H)/(S + H)$, where *S*, *M* and *H* correspond to the net counts in the soft, medium and hard bands, respectively. We give the results of the analysis in Table 2, where the counts in the 0.5–7 keV band, the hardness ratios and the absorbed (F_x^{Abs}) and corrected (F_x^{Cor}) fluxes are shown. In the last column, the absorbed (L_x^{Abs}) and corrected luminosity (L_x^{Cor}) of each source

³ In the case of point-like sources, the aperture radius was $\approx 1.3''$, which corresponds to an encircled energy of $\approx 90\%$ at 1.4 keV.

Table 2. Properties of the observed discrete sources in NGC 6388 (see text for the source 14*).

Source	Net (counts) (0.5–7 keV)	HR1 (S – M)/(S + M)	HR2 (M – H)/(M + H)	HR3 (S – H)/(S + H)	F_x^{Abs} (F_x^{Cor}) ($\times 10^{-14}$ cgs)	L_x^{Abs} (L_x^{Cor}) ($\times 10^{32}$ cgs)
1	172.0 ± 13.3	0.26 ± 0.09	0.20 ± 0.09	–0.06 ± 0.10	2.9 (3.7)	4.6 (5.8)
2	195.1 ± 14.2	–0.18 ± 0.11	–0.52 ± 0.07	–0.38 ± 0.07	3.3 (4.2)	5.2 (6.6)
3	527.1 ± 23.0	0.53 ± 0.04	0.96 ± 0.01	0.86 ± 0.04	8.9 (11.2)	14.0 (17.6)
4	37.0 ± 6.3	–0.12 ± 0.20	–0.04 ± 0.21	0.08 ± 0.20	0.6 (0.8)	0.9 (1.2)
5	125.1 ± 11.4	0.80 ± 0.06	0.95 ± 0.03	0.60 ± 0.21	2.1 (2.7)	3.3 (4.2)
6	41.9 ± 6.8	–0.04 ± 0.19	–0.07 ± 0.20	–0.03 ± 0.20	0.7 (0.9)	1.1 (1.4)
7	134.7 ± 11.9	0.66 ± 0.07	0.89 ± 0.04	0.57 ± 0.16	2.3 (2.9)	3.6 (4.6)
8	87.0 ± 9.8	0.30 ± 0.13	0.18 ± 0.13	–0.12 ± 0.16	1.4 (1.8)	2.2 (2.8)
9	109.0 ± 10.6	0.25 ± 0.11	0.27 ± 0.11	0.02 ± 0.13	1.8 (2.3)	2.8 (3.6)
10	355.0 ± 19.1	0.54 ± 0.05	0.97 ± 0.02	0.91 ± 0.03	6.0 (7.6)	9.4 (11.9)
11	78.1 ± 8.8	–0.23 ± 0.13	0.02 ± 0.15	0.25 ± 0.13	1.3 (1.6)	2.0 (2.5)
12	108.1 ± 10.7	–0.18 ± 0.13	–0.11 ± 0.14	0.07 ± 0.12	1.8 (2.3)	2.8 (3.6)
13	127.8 ± 11.7	0.14 ± 0.10	0.30 ± 0.11	0.17 ± 0.12	2.2 (2.7)	3.4 (4.2)
14*	789.6 ± 28.8	0.38 ± 0.04	0.58 ± 0.03	0.26 ± 0.06	13.4 (16.8)	21.1 (26.5)

(in the 0.5–7 keV) has been determined assuming a $\Gamma = 1.7$ power law absorbed by the Galactic line-of-sight column density $N_{\text{H}} \approx 2.5 \times 10^{21} \text{ cm}^{-2}$.

The three sources (labeled as 14*) present in the globular cluster center should be viewed cautiously: since we cannot resolve them in a better way we refer to the cumulative net counts and luminosity.

3. The inner X-ray cluster in NGC 6388

As we have seen in the previous section, the better angular resolution of the *Chandra* satellite with respect to that of *XMM*-Newton, allowed us to detect several discrete sources within a few core radii of NGC 6388. The main properties of the detected sources are given in Table 2.

Any classification of the detected sources requires an understanding of their spectral shapes. Due to the low count rates of most of the detected sources, formal spectral modeling is only possible for the brightest ones (namely those with more than 300 counts and labeled as 3, 10 and 14*).

For the other sources, a rough classification can be done by using a color–color diagram (see Fig. 5) in which the two hardness ratios $\text{HR}_{\text{soft}} = (M - S)/(S + M + H)$ and $\text{HR}_{\text{hard}} = (H - M)/(S + M + H)$ are given. In the same plot, we give the expected set of color–color contours for bremsstrahlung (grey region) and power law (black region) components, respectively. In both the two regions, the equivalent hydrogen column N_{H} (taken varying between 10^{20} cm^{-2} and 10^{22} cm^{-2}) is associated with almost horizontally-oriented lines. The temperature kT of the bremsstrahlung models (taken in the range 0.1–2.5 keV) is associated with primarily vertical-lines. In the case of the power law region, vertical orientation is associated with values of the parameter Γ in the range 0.1–2.5.

According to the classification scheme of Jenkins et al. (2005), to which we refer for more details, most of the sources with $\text{HR}_{\text{soft}} \gtrsim -0.2$ seem to be low mass X-ray binaries, with the source 2 possibly being a high mass X-ray binary containing a neutron star.

The source labeled as 14* is positioned in a region of the color-color diagram where its spectral properties are not well fitted by a single spectral component (represented by the two shaded regions), even if it seems marginally consistent with power law models with large exponents (Γ greater than 2.5, typical of X-ray emission from IMBHs, which are expected to be soft sources). This was expected since we extracted the

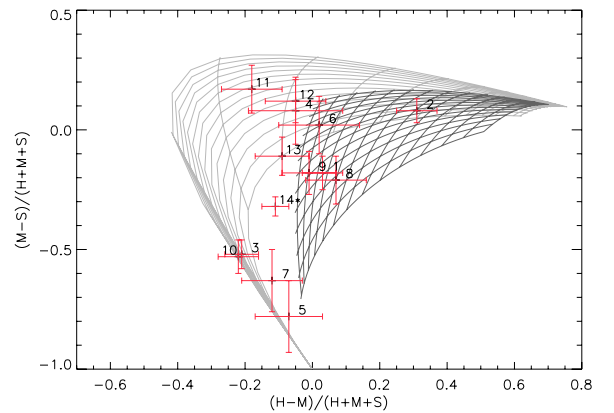


Fig. 5. Color–color diagram of the sources (data points) detected within a few core radii in NGC 6388 and color–color contours for bremsstrahlung (grey region) and power law (black region) components, respectively. On the horizontal and vertical axes, the two hardness ratios $\text{HR}_{\text{hard}} = (H - M)/(S + M + H)$ and $\text{HR}_{\text{soft}} = (M - S)/(S + M + H)$ are given (see text for details). (This figure is available in color in electronic form.)

cumulative spectrum of what appeared to be the superposition of three different sources (possibly LMXRBs), each of which has different spectrum properties. Finally, note the existence of four soft sources corresponding to $\text{HR}_{\text{soft}} \lesssim -0.5$.

Interestingly, the cumulative luminosity of the sources detected in the *Chandra* field of view (see Table 2) is fully consistent with that derived by the *XMM*-Newton observation of NGC 6388. For the three sources with more than 300 counts (3, 10 and 14*) detected within the NGC 6388 globular cluster, we extracted the spectrum from a circular aperture centered on each of the three sources. Note that the source labeled as 14* seems to be the superposition of three distinct sources (see also the true color images in Fig. 3), for which it was not possible to extract the single spectra. In this case we refer to the cumulative spectrum.

The spectra (shown in Fig. 6) were rebinned with 25 counts per bin and fitted using the XSPEC spectral fitting package. All the errors given below are at a 90% confidence level.

The spectrum of the source 3 is well fitted ($\chi^2/\nu = 0.76$ for $\nu = 15$) by an absorbed black-body model with temperature $kT = 0.26^{+0.03}_{-0.10}$ keV, hydrogen column density $N_{\text{H}} = 3.1^{+0.1}_{-0.1} \times 10^{21} \text{ cm}^{-2}$, and normalization $N = 1.2^{+0.6}_{-0.3} \times 10^{-7}$

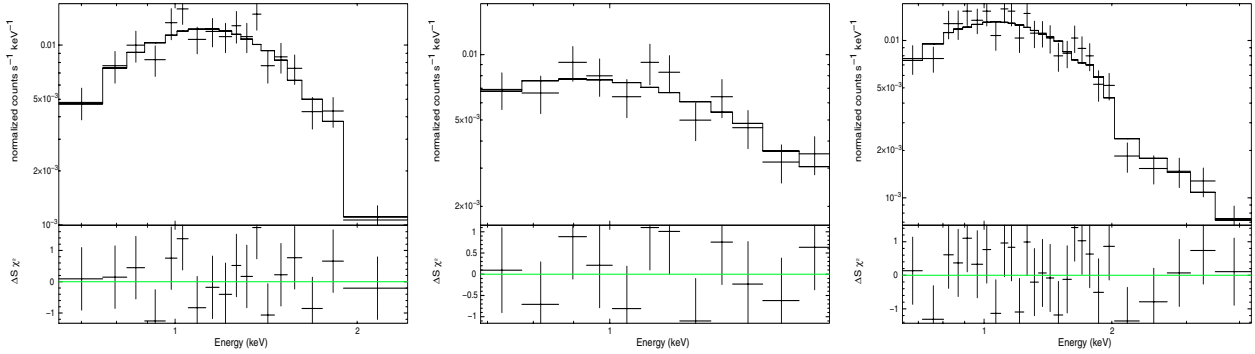


Fig. 6. The spectra of the sources labeled as 3, 10 and 14* from the left to the right (see text for details on the fit). (This figure is available in color in electronic form.)

corresponding to a flux (in the 0.5–7 keV) of 4.5×10^{-14} erg cm $^{-2}$ s $^{-1}$.

Source 10 is characterized by a power law whose best fit parameters ($\chi^2/\nu = 0.76$ for $\nu = 9$) are $N_{\text{H}} = 1.6^{+1.7}_{-1.6} \times 10^{21}$ cm $^{-2}$, $\Gamma = 2.4^{+1.3}_{-1.0}$ and $N = 2.0^{+0.3}_{-0.9} \times 10^{-5}$ for the column density, power law index and normalization, respectively. The derived flux in the 0.5–7 keV is $5.1^{+0.2}_{-3.6} \times 10^{-14}$ erg cm $^{-2}$ s $^{-1}$.

As discussed above, the source labeled as 14* seems to be the superposition of three different sources: one very soft and the other two harder, which lie close to the center of gravity of the globular cluster. With the present observations there is no way to discriminate whether one of these X-ray sources is associative with the IMBH hosted in NGC 6388. Nevertheless, if this is the case, the observed flux in the 0.5–7 keV can be considered as the present upper limit to the IMBH X-ray signal. The source appears to be soft since the best fit absorbed power law ($\chi^2/\nu = 0.81$ for $\nu = 26$) has parameters $N_{\text{H}} = 2.7^{+0.05}_{-0.1} \times 10^{21}$ cm $^{-2}$, $\Gamma = 2.4^{+0.3}_{-0.2}$ and $N = 4.7^{+1.4}_{-0.6} \times 10^{-5}$ for the column density, power law index and normalization, respectively. In this case, the flux in the 0.5–7 keV would be 1.02×10^{-13} erg cm $^{-2}$ s $^{-1}$ corresponding to an X-ray luminosity of 2.7×10^{33} erg s $^{-1}$.

4. Results and conclusions

Intermediate-mass black holes may represent the link between the stellar mass black holes present throughout the Milky Way and the super-massive black hole thought to exist in the center of the Galaxy and in external galaxies. Recent theoretical works have suggested that all the globular clusters may have central black holes with masses of the order 10^{-3} times the stellar mass in the cluster, as a consequence of merging processes of stellar mass black holes (Miller & Hamilton 2002). Present observational campaigns seem to confirm this hypothesis.

In the particular case of NGC 6388, numerical simulations (see e.g. Baumgardt et al. 2005) have shown that it is a good candidate to host an IMBH of a few $10^3 M_{\odot}$. Interestingly, the optical HST observations of the globular cluster and the detailed study of the brightness surface profile down to a distance of $\approx 1''$ from the center, revealed a significant power law (with slope $\alpha \approx -0.2$) deviation from a flat core behavior (Lanzoni et al. 2007). This was explained assuming the existence of an IMBH with mass $5.7 \times 10^3 M_{\odot}$ in the center of the globular cluster.

As a consequence of matter accretion, we expect that the putative IMBH should accrete and emit radiation in the X-ray band, so we searched for such a signature in the observations available in both *XMM-Newton* and *Chandra* archives.

The study of the central region of NGC 6388 in the 0.5–7 keV energy band reveals the existence of several discrete X-ray sources (see Sect. 3 for a detailed discussion) among which three of them seem to be overlapped and close to the center of gravity of NGC 6388. Although we can not obtain the spectrum of each of the three sources separately, we have speculated that if one of these is the putative NGC 6388 IMBH, the observed X-ray signal can be thought as an upper limit to the IMBH flux.

Hence, with reference to Table 2, the unabsorbed X-ray flux (in the 0.5–7 keV band) of the IMBH is $F_{\text{X}}^{\text{Obs}} \lesssim 1.6 \times 10^{-13}$ erg cm $^{-2}$ s $^{-1}$, corresponding to a luminosity of $L_{\text{X}}^{\text{Obs}} \lesssim 2.7 \times 10^{33}$ erg s $^{-1}$ for the NGC 6388 distance of 11.5 kpc.

At this point one can evaluate the IMBH radiative efficiency $\eta = L_{\text{X}}/L_{\text{Edd}}$ with respect to the maximum allowed black hole accretion rate given by the Eddington luminosity $L_{\text{Edd}} \approx 1.38 \times 10^{38} (M/M_{\odot})$ erg s $^{-1}$. For the IMBH at the center of NGC 6388 one gets $L_{\text{Edd}} \approx 7.87 \times 10^{41}$ erg s $^{-1}$, so that we can conclude that it is accreting with efficiency $\eta \lesssim 3 \times 10^{-9}$. Note that this accretion efficiency is in agreement with the efficiency estimates for black hole accretion in quiescent galaxies and ultra-low luminous AGNs, for which η is typically in the range $4 \times 10^{-12} - 6 \times 10^{-7}$ (Baganoff et al. 2003).

The bolometric luminosity of the NGC 6388 IMBH can be inferred from the broadband spectral energy distributions of galactic nuclei (see Elvis et al. 1994, for details). In this case, it is found that the bolometric correction for the X-ray band corresponds to a factor $\sim 7-20$, so that $L_{\text{bol}}/L_{\text{Edd}} \lesssim (2-6) \times 10^{-8}$ (or $L_{\text{bol}} \lesssim (2-5) \times 10^{34}$ erg s $^{-1}$).

It could be also interesting to estimate the expected accretion luminosity (L_{acc}) of the IMBH as a consequence of the accretion of the surrounding gas, and compare it to the bolometric luminosity (L_{bol}) above. It is indeed expected that post-main-sequence stars continuously lose mass that is injected both in the cluster and intracluster medium. Dispersion measurements derived from radio observations of pulsars give the most sensitive probe of the gas content in globular clusters. Studying the population of millisecond pulsars in the globular clusters M 15 and 47 Tuc, Freire et al. (2001) find indications of the presence of a plasma with electron density $n_{\text{e}} \approx 0.2$ atoms cm $^{-3}$ and temperature $T \approx 10^4$ K (see also Ho et al. 2003, for a detailed study of the M 15 globular cluster). In common with other authors (Maccarone 2004), we assume in the following that the gas density in NGC 6388 is ~ 0.2 atoms cm $^{-3}$. If the IMBH at the center of NGC 6388 accretes spherically through the Bondi accretion process, the gravitational potential of the IMBH dominates the dynamics of the gas within the accretion radius defined as

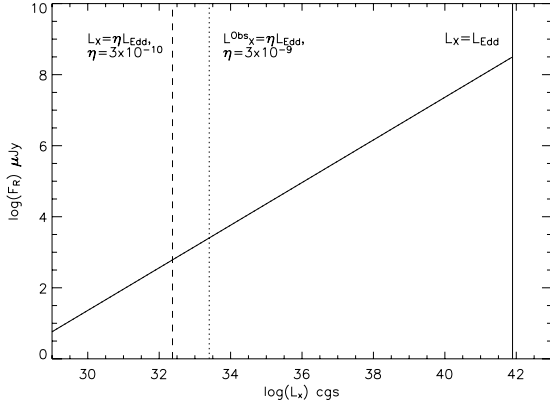


Fig. 7. The expected radio emission (solid oblique line) from the IMBH at the center of NGC 6388 as a function of the IMBH X-ray luminosity. Present X-ray observations can put only an upper limit of ≈ 3 mJy to the black hole radio luminosity.

$R_a \approx GM_{\text{bh}}/c_s^2$, where $c_s \approx 0.1T^{1/2}$ km s $^{-1}$ is the sound speed in a plasma at temperature T . For $T = 10^4$ K and $M_{\text{bh}} = 5.7 \times 10^3 M_{\odot}$, one obtains $c_s \approx 10$ km s $^{-1}$ and $R_a \approx 0.3$ pc. The accretion mass rate in the Bondi mechanism is $\dot{M}_B = 4\pi R_a^2 \rho_a c_s$, where ρ_a is the gas density at R_a . Assuming that the efficiency in converting the accreted mass into energy is the standard $\epsilon = 10\%$, the expected luminosity due to accretion is $L_{\text{acc}} = \epsilon \dot{M}_B c^2$, i.e.

$$L_{\text{acc}} = 2.4 \times 10^{38} \left(\frac{\epsilon}{0.1} \right) \times \left(\frac{M_{\text{bh}}}{5.7 \times 10^3 M_{\odot}} \right)^2 \left(\frac{n}{0.2 \text{ cm}^{-3}} \right) \left(\frac{c_s}{10 \text{ km s}^{-1}} \right)^{-3} \text{ cgs.} \quad (1)$$

Hence, in the case of the NGC 6388 IMBH, the accretion luminosity is clearly larger than the bolometric luminosity quoted above by a factor of at least $\approx 10^4$, leading us to conclude that the accretion efficiency is $\epsilon \lesssim 8 \times 10^{-5} - 2 \times 10^{-4}$.

In recent years it has also been proposed that a relationship between black hole mass, X-ray luminosity and radio luminosity does exist (see e.g. Merloni et al. 2003; and Maccarone 2004). In this context, IMBHs at the center of many globular clusters, such as NGC 6388, may be easily identifiable objects in deep radio observations.

In particular, the expected radio flux at 5 GHz from the putative IMBH in NGC 6388 would be

$$F_5 = 10 \left(\frac{L_X}{3 \times 10^{31} \text{ cgs}} \right)^{0.6} \left(\frac{M_{\text{bh}}}{100 M_{\odot}} \right)^{0.78} \left(\frac{10 \text{ kpc}}{d} \right)^2 \mu\text{Jy.} \quad (2)$$

Assuming that it is a quiescent and stable accreting black hole, we can be more predictive about its radio luminosity. In Fig. 7,

the expected radio emission (solid oblique line) from the IMBH at the center of NGC 6388 is shown. The solid vertical line represents the maximum allowed X-ray luminosity for an Eddington limited accreting black hole. As one can see, depending on the accretion efficiency (dotted and dashed lines are for $\eta = 3 \times 10^{-9}$ and $\eta = 3 \times 10^{-10}$, respectively) the radio flux at 5 GHz is $\lesssim 3$ mJy, which is within the detection possibilities of the Australia Telescope Compact Array (ATCA). Deep radio observations within the core radius of NGC 6388 would also be important for the possibility of discovering millisecond pulsars nearby the cluster center that may allow a further and independent constraint on the IMBH mass and position with respect to the cluster center⁴.

Acknowledgements. This paper is based on observations from *XMM-Newton*, an ESA science mission with instruments and contributions directly funded by ESA member states and NASA. We are grateful to G. Trinchieri and L. Bello for useful discussions. We are grateful to the anonymous referee for the suggestions that improved the manuscript.

References

- Baganoff, F. K., Maeda, Y., Morris, M., et al. 2003, *ApJ*, 591, 891
Bahcall, J. N., & Wolf, R. A. 1976, *ApJ*, 209, 214
Baumgardt, H., Makino, J., Hut, Piet, McMillan, S., & Portegies Zwart, S. 2003, *ApJ*, 589, 25
Baumgardt, H., Hut, P., Makino, J., McMillan, S., Portegies Zwart, S. 2003, *ApJ*, 582, L21
Baumgardt, H., Makino, J., & Hut, P., 2005, *ApJ*, 620, 238
Dickey, J. M., & Lockman, F. J. 1990, *ARA&A*, 28, 215
De Paolis, F., Gurzadyan, V. G., & Ingrassio, G. 1996, *A&A*, 315, 396
Elvis, M., Wilkes, B. J., McDowell, J. C., et al. 1994, *ApJS*, 95, 1
Freire, P. C., Kramer, M., Lyne, A. G., et al. 2001, *ApJ*, 557, L105
Gebhardt, K., Rich, R. M., & Ho, L. C. 2002, *ApJ*, 578, L41
Gebhardt, K., Rich, R. M., & Ho, L. C. 2005, *ApJ*, 634, 1093
Gerssen, J., van der Marel, R., Gebhardt, K., et al. 2002, *AJ*, 124, 3270
Gerssen, J., van der Marel, R. P., Gebhardt, K., et al. 2003, *AJ*, 125, 376
Giacconi, R., Rosati, P., Tozzi, P., et al. 2001, *ApJ*, 551, 624
Gurzadyan, V. G. 1982, *A&A*, 114, 71
Harris, W. E. 1996, *AJ*, 112, 1487
Ho, L. C., Terashima, Y., & Okajima, T. 2003, *ApJ*, 587, L35
Lanzoni, B., Dalessandro, E., Ferraro, F. R., et al. 2007, *ApJ*, 668, L139
Jenkins, L. P., Roberts, T. P., Warwick, R. S., Kilgard, R. E., & Ward, M. J. 2005, *MNRAS*, 357, 401
Maccarone, T. J. 2004, *MNRAS*, 351, 1049
Miller, M. C., & Colbert, E. 2003, *IJMP D*, 13, 1
Miocchi, P. 2007, *MNRAS*, 381, 103
Magorrian, J., Tremaine, S., Richstone, D., et al. 1998, *AJ*, 115, 2285
Merloni, A., Heinz, S., & Di Matteo, T. 2003, *MNRAS*, 345, 1057
Merritt, D., Berczik, P., & Laun, F. 2007, *AJ*, 133, 533
Miller, M. C., & Hamilton, D. P. 2002, *MNRAS*, 330, 232
Noyola, E., & Gebhardt, K. 2006, *AJ*, 132, 447
Pooley, D., & Rappaport, S. 2006, *ApJ*, 644, L45
Portegies Zwart, S. F., Baumgardt, H., Hut, P., Makino, J., & McMillan, S. L. W. 2004, *Nature*, 428, 724
Strüder, L., Briel, U., Dennerl, K., et al. 2001, *A&A*, 365, L18
Turner, M. J. L., Abbey, A., Arnaud, M., et al. 2001, *A&A*, 365, L27

⁴ Indeed, one expects that an IMBH randomly moves, within the globular cluster core, due to the interaction with the other stars (assumed to have the same mass m) with an amplitude $\sim r_c(m/M_{\text{bh}})$ (see e.g. Bahcall & Wolf 1976; Gurzadyan 1982; and Merritt et al. 2007).